Chemistry changes with size

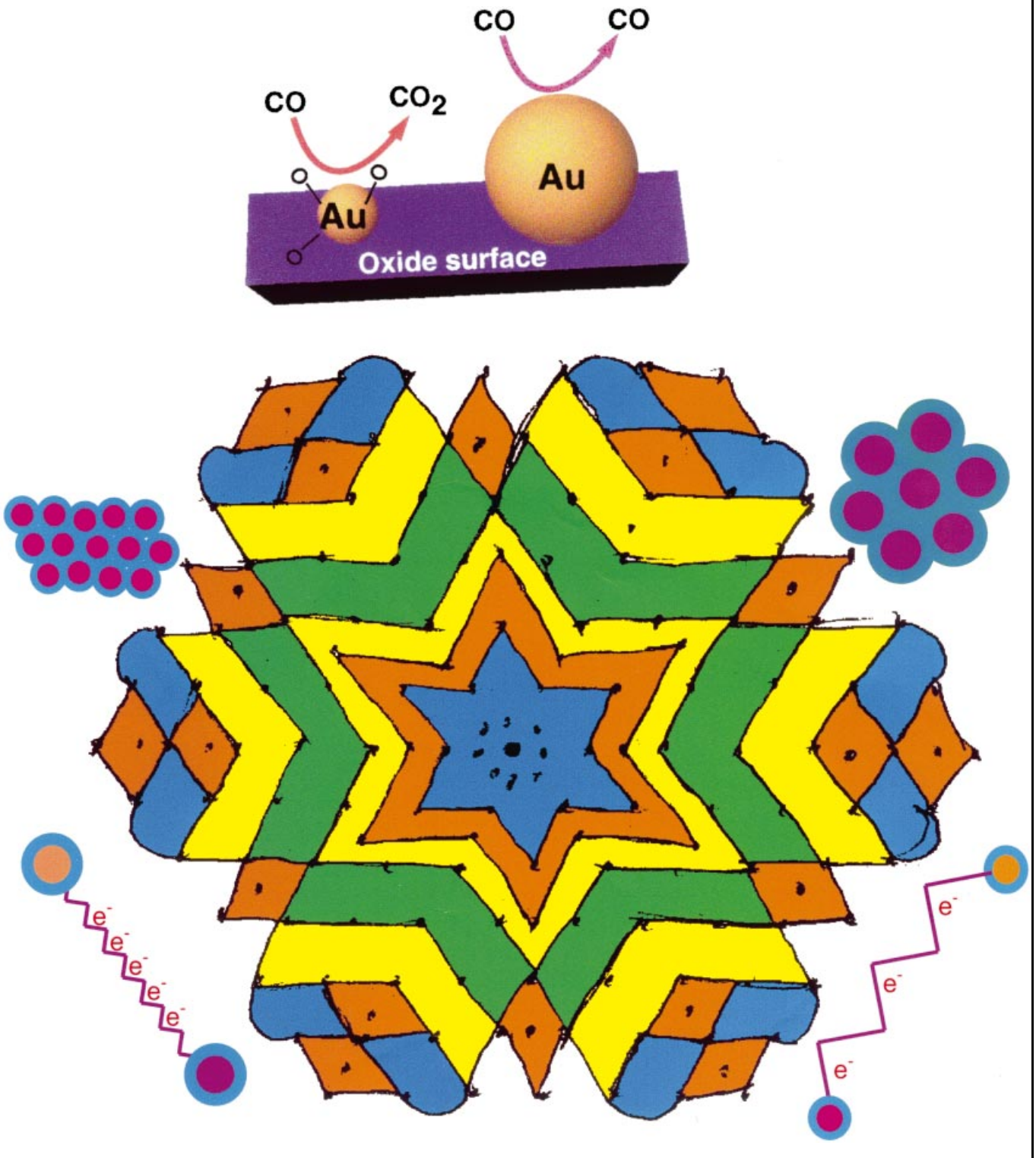

The picture shows a traditional Indian *rangoli* filled with colors of differently sized CdSe nanoparticles. Schematic illustrations of size dependent reactivity, self-assembled two-dimensional arrays and Coulomb staircases adorn the *rangoli*.

0947-6539/02/0801-0028 $ 17.50+.50/0 *Chem. Eur. J.* **2002**, *8*, No. 1

Size-Dependent Chemistry: Properties of Nanocrystals

C. N. R. Rao,*[a] G. U. Kulkarni,[a] P. John Thomas,[a] and Peter P. Edwards*[b]

Abstract: Properties of materials determined by their size are indeed fascinating and form the basis of the emerging area of nanoscience. In this article, we examine the size dependent electronic structure and properties of nanocrystals of semiconductors and metals to illustrate this aspect. We then discuss the chemical reactivity of metal nanocrystals which is strongly dependent on the size not only because of the large surface area but also a result of the significantly different electronic structure of the small nanocrystals. Nanoscale catalysis of gold exemplifies this feature. Size also plays a role in the assembly of nanocrystals into crystalline arrays. While we owe the beginnings of size-dependent chemistry to the early studies of colloids, recent findings have added a new dimension to the subject.

Keywords: colloids · nanostructures · self-assembly · semiconductors

Introduction

Steric effects—arising from bulky groups—are well known as key factors in determining the reactivity of organic molecules. Otherwise, we do not ordinarily concern ourselves with the physical dimension of a system as a factor in determining its intrinsic properties except in intercalation chemistry or some such situation where the pore or cavity in a host lattice molecule can accommodate guest species of a particular size. Size, however, becomes *the* sole controlling factor while dealing with the science and application of the so-called nanoparticles, that cover a size range between 1 – 100 nm. Nanoparticles within this size domain are thus intermediate between the atomic and molecular size regimes on one hand, and the macroscopic, bulk on the other. In this regime, size-dependent properties manifest themselves when the size of an individual particle is sufficiently small. A key aspect of the rapidly developing area of nanoscience and nanotechnology concerns itself with the size dependence of intrinsic properties of materials. It is, therefore, instructive to look at typical properties of metals and semiconductors in the size-dependent regime of nanoparticles. We shall discuss three important aspect of the nanocrystals of these materials, electronic structure and properties, chemical reactivity and self-assembly. Size dependent structural and thermodynamic properties of nanoparticles such as bond lengths, melting point and specific heat have already been reviewed[1] in the literature and will not be discussed in any detail in the present article.

Two centuries ago the study of nanoscale solid particles, dispersed within a liquid host, played a pivotal role in establishing colloid science. During the final decades of the last century, colloid science was, perhaps, something of an intellectual backwater—with one or two notable exceptions. However, significant advances in both experimental and theoretical aspects of the subject, and, of course, the emergence of, and explosion of interest in, the broad area of nanoscience and nanotechnology, have now set the scene for a renaissance in colloid science. Interestingly, it does appear that many scientists in the modern field of nanoscience may not even recognize its colloidal source. This is unfortunate, since there is a wealth of information and expertise in that old and venerable science.

An important example of the parentage of the modern subject of metal nanoparticles derives from the work of Faraday in the 1850s. During that period, Faraday carried out groundbreaking studies of nanoscale gold particles in aqueous solution. He established the first quantitative basis for the area, noting that these colloidal metal sols ("pseudosolutions") are thermodynamically unstable, and that the individual gold nanoparticles must be stabilized kinetically against aggregation. Once the nanoparticles coagulate, the process cannot be reversed. Remarkably, Faraday also identified the very essence of the nature of colloidal, nanoscale particles of metals; specifically, for the case of gold, he concluded (in

[a] Prof. Dr. C. N. R. Rao, Prof. Dr. G. U. Kulkarni, P. J. Thomas
Chemistry and Physics of Materials Unit
Jawaharlal Nehru Center for Advanced Scientific Research
Jakkur P.O., Bangalore, 560 064 (India)
E-mail: cnrrao@jncasr.ac.in

[b] Prof. Dr. P. P. Edwards
School of Chemistry
University of Birmingham, Edgbaston,
Birmingham, B15 2TT (UK)
E-mail: p.p.edwards@bham.ac.uk

  0947-6539/02/0801-0029 $ 17.50+.50/0

1857!) … "*the gold is reduced in exceedingly fine particles which becoming diffused, produce a beautiful fluid … the various preparations of gold whether ruby, green, violet or blue … consist of that substance in a metallic divided state*".

During that century, colloidal phenomena played a pivotal role in the genesis of physical chemistry by establishing a connection between descriptive chemistry and theoretical physics. For example, Einstein provided the relationship between Brownian motion and diffusion coefficient of colloidal particles.

Today, the overwhelming importance now associated with the nanoscale in both science and technology means that the scene is once again set for this key subject to impact upon the development of not only chemistry, but also physics and materials science. In the following sections we attempt to highlight a few of the key issues relating to nanparticles where size determines their properties.

Electronic structure and properties: The electronic structure of a nanocrystal critically depends on its very size. For small particles, the electronic energy levels are not continuous as in bulk materials, but discrete, due to the confinement of the electron wavefunction because of the physical dimensions of the particles (see Figure 1). The average electronic energy level spacing of successive quantum levels, δ, known as the so-called Kubo gap, is given by, $\delta = 4E_f/3n$, where E_f is the Fermi energy of the bulk material and n is total number of valence electrons in the nanocrystal. Thus, for an individual silver nanoparticle of 3 nm diameter containing approximately one thousand silver atoms, the value of δ would be 5 – 10 meV. Since the thermal energy at room temperature, $kT \cong 25$ meV, a 3 nm particle would be metallic ($kT > \delta$). At low temperatures, however, the level spacings specially in small particles, may become comparable to kT, rendering them nonmetallic.[2] Because of the presence of the Kubo gap in individual nanoparticles, properties such as electrical conductivity and magnetic susceptibility exhibit quantum size effects.[3] The resultant discreteness of energy levels also brings about fundamental changes in the characteristic spectral features of the nanoparticles, especially those related to the valence band.

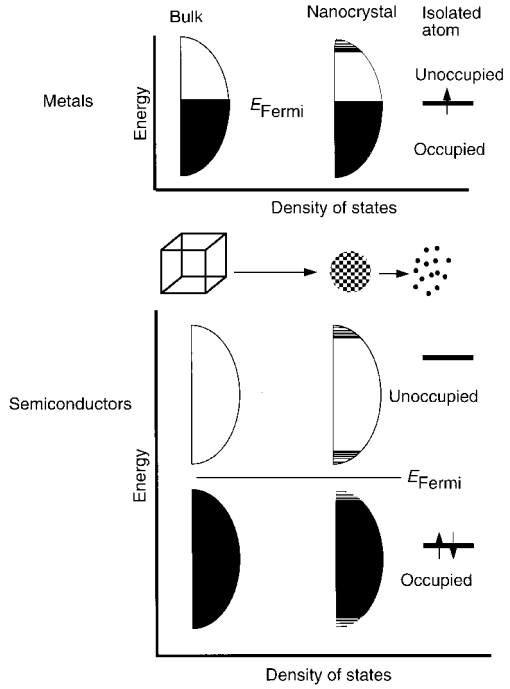

Figure 1. Density of states for metal (a) and semiconductor (b) nanocrystals. In each case, the density of states is discrete at the band edges. The Fermi level is in the center of a band in a metal, and so kT may exceed the electronic energy level spacing even at room temperatures and small sizes. In contrast, in semiconductors, the Fermi level lies between two bands, so that the relevant level spacing remains large even at small sizes. The HOMO – LUMO gap increases in semiconductor nanocrystals of smaller sizes.

Extensive investigations of metal nanocrystals of various sizes obtained, for example by the deposition of metals on amorphised graphite and other substrates, by X-ray photoelectron spectroscopy and related techniques[4, 5] have yielded valuable information on their electronic structure. An important result from these experiments is that as the metal particle size decreases, the core-level binding energy of metals such as Au, Ag, Pd, Ni and Cu increases sharply. This is shown in the case of Pd in Figure 2, where the binding energy

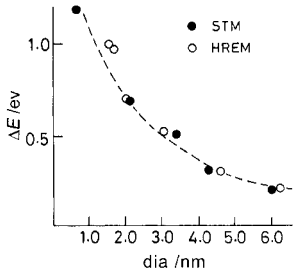

Figure 2. Variation of the shift, ΔE, in the core-level binding energy (relative to the bulk metal value) of Pd with the nanoparticle diameter. The diameters were obtained from HREM and STM images (reproduced with permission from ref. [3]).

increases by over 1 eV at small size. The variation in the binding energy is negligible at large coverages or particle size, since the binding energies are close to those of the bulk, macroscopic metals. The increase in the core-level binding energy in small particles occurs due to the poor screening of the core-hole and is a manifestation of the *size-induced metal-nonmetal transition* in nanocrystals. Further evidence for the occurrence of such a metal-nonmetal transition driven by the size of the individual particle is provided by other electron spectroscopic techniques such as UPS, BIS.[5–7] All these measurements indicate that an electronic gap manifests itself for a nanoparticle having diameters of 1 – 2 nm possessing 300 ± 100 atoms.

Photoelectron spectroscopic measurements[6] on mass-selected Hg_n nanoparticles ($n = 3$ to 250) in the gas phase reveal that the characteristic HOMO – LUMO (s – p) energy gap decreases gradually from $\sim$3.5 eV for $n = 3$ to $\sim$0.2 eV for $n =$ 250, as shown in Figure 3. The band gap closure is predicted at $n \sim 400$. The metal – nonmetal transition in gaseous Hg nanoparticles was examined by Rademann and co-workers[7] by measuring the ionization energies (IE). For $n < 13$, the dependence of IE on n suggested a different type of bonding. A small Hg particle with atoms in the $6s^26p^0$ configuration

0947-6539/02/0801-0030 $ 17.50+.50/0 *Chem. Eur. J.* **2002**, *8*, No. 1

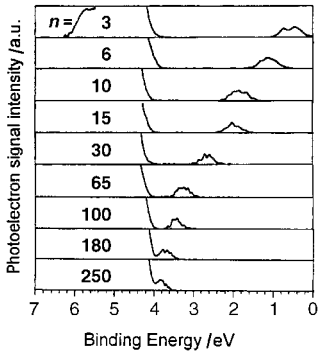

Figure 3. Photoelectron spectra of Hg clusters of varying nuclearity. The 6p feature moves gradually towards the Fermi level, emphasizing that the band gap shrinks with increase in cluster size (reproduced with permission from ref. [6]).

held together by relatively weak van der Waals forces, is essentially nonmetallic. As the nanoparticle grows in size, the atomic 6s and 6p levels broaden into bands and an insulator–metal transition appears to occur—driven by the physical dimensions of the individual particle. Note that this is the same element, Hg, behaving as either a metal or a nonmetal, depending upon its physical size!

The electronic absorption spectrum of metal nanocrystals in the visible region is dominated by the plasmon band. This absorption is due to the collective excitation of the itinerant electron gas on the particle surface and is characteristic of a metal nanocrystal of the given size. In colloids, surface plasmon excitations impart characteristic colours to the metal sols, the beautiful wine-red colour of gold sols being well-known. Gold nanocrystals of varying diameters between 2 and 4 nm exhibit distinct bands around $\sim$525 nm, the intensity of which increases with size.[9, 10] The intensity of this feature becomes rather small in the case of 1 nm diameter particles basically due to a reduced less number of "itinerant" electrons in the electron cloud. With a change in temperature, the intensity of the plasmon band decreases as seen in the case of Au nanocrystals.[10] In contrast to the situation for metals, exciton peaks dominate the absorption of semiconductor nanocrystals in the visible region.[11, 12a] Thus CdS, a yellow solid, exhibits an exciton peak around 600 nm, which gradually shifts into the UV region as the nanocrystal diameters are varied below 10 nm (see Figure 4).[12b] Similar effects have been observed in the case of PbS and ZnO.[12b]

Direct information on the gap states in nanocrystals of metals and semiconductors is obtained by scanning tunneling spectroscopy (STS). This technique provides the desired sensitivity and spatial resolution making it possible to carry out tunneling spectroscopic measurements on individual particles. A systematic STS study of Pd, Ag, Cd and Au nanoparticles of varying sizes deposited on a graphite substrate has been carried out under ultrahigh vacuum conditions, after having characterized the nanoparticles by XPS and STM.[13] The I-V spectra of bigger particles were featureless while those of the small particles (<1 nm) showed well-defined peaks on either side of zero-bias due to the presence of a gap. Ignoring gap values below 25 meV ($\sim kT$), it is seen that small particles of ≤ 1 nm diameter are in fact

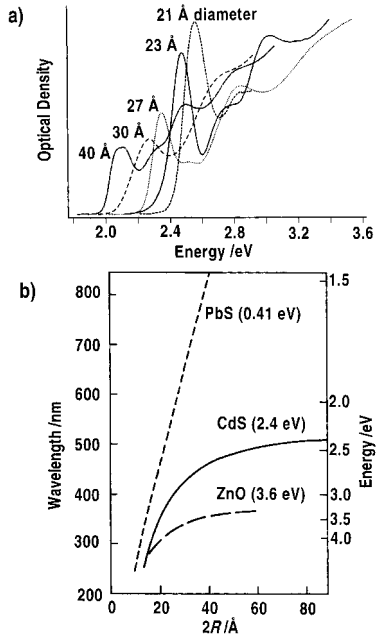

Figure 4. a) Absorption spectra of CdSe nanocrystals (at 10 K) of various diameters (reproduced with permission from ref. [12a]). b) Wavelength of the absorption threshold and band gap as a function of the particle diameter for various semiconductors. The corresponding energy gap in the bulk state is given in parenthesis (reproduced with permission from ref. [12b]).

nonmetallic! (Figure 5a) From the various studies discussed hitherto, it appears that the size-induced metal–insulator transition in metal nanocrystals (Figure 1) occurs in the range of 1–2 nm diameter or 300 ± 100 atoms. The band gap of CdS nanocrystals estimated by the above method yielded a value of 2.9 eV for a 3.1 nm diameter nanocrystal[14] and the gap increases with the decrease in size (Figure 5b).

Theoretical calculations of the electronic structure of metal and semiconductor nanocrystals throw light on the size-

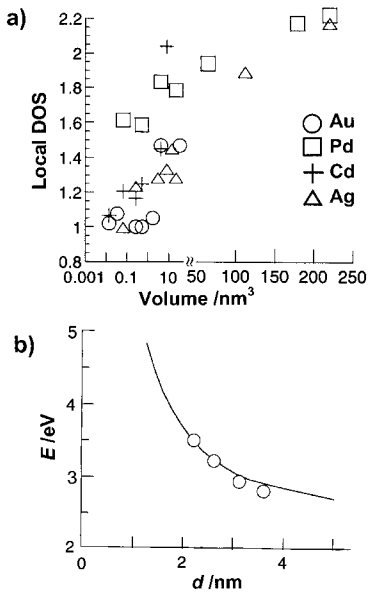

Figure 5. a) Variation of the nonmetallic band gap with nanocrystal size, b) in CdS nanocrystals (reproduced with permission from refs. [13, 14]).

induced changes in the electronic structure. Rosenblit and Jortner[15] calculated the electronic structure of a model metal cluster and predicted electron localization to occur in a cluster of diameter ~0.6 nm. A molecular orbital calculation on Au_{13} cluster[16] in icosahedral and cuboctahedral structures shows that the icosahedral structure undergoes Jahn–Teller distortion while the cuboctahedral structure does not distort. The onset of the metallic state is barely discernible in the Au_{13} cluster. Relativistic density functional calculations of gold clusters,[17] with $n = 6$ to 147 show that the average interatomic distance increases with the nuclearity of the cluster. The HOMO–LUMO electronic gap decreases with particle size from 1.8 eV for Au_6 (~0.5 nm diameter) to 0.3 eV for Au_{147} (~2 nm diameter). Ab initio molecular dynamics simulations of aluminum clusters,[18] with $n = 2-6$, 12, 13, 55 and 147 reveal that the minimum energy structures of Al_{13} and Al_{55} to be distorted icosahedra whereas Al_{147} is a near cuboctahedron. The HOMO–LUMO gap increases from ~0.5 eV for Al_2 to ~2 eV for Al_{13}; the gap is around 0.25 eV for Au_{55} and decreases to ~0.1 eV for Au_{147}. In the case of semiconductor nanocrystals, it is shown using tight binding approximation that the band gaps nearly reach the bulk values at sizes of around 5 nm.[19] The convergence of the cluster properties towards those of the corresponding bulk materials with increase in size is noteworthy.

In a bulk metal, the energy required to add or remove an electron is its work function. In a molecule, the corresponding energies, electron affinity and ionization potential, respectively, are, however, nonequivalent. Nanocrystals being intermediary, the two energies differ only to a small extent,[20] the difference being the charging energy, *U*. This is a Coulombic energy and is different from electronic energy gap. Further, Coulombic states can be similar for both semiconductor and metallic nanocrystals unlike the electronic states. A manifestation of single electron charging is the Coulomb staircase behaviour observed in the tunneling spectra,[21] when a nanocrystal, covered with an insulating ligand shell is held between two tunnel junctions. A typical staircase along with its theoretical fit is shown in Figure 6a. Such measurements have also been carried out on Pd and Au nanocrystals in the size range, 1.5–6.5 nm.[22] The charging energies follow a scaling law[23] of the form, $U = A + B/d$, where A and B are constants, characteristic of the metal and *d* is the particle diameter(see Figure 6b).

Magnetic properties of nanoparticles of transition metals such as Co, Ni show marked variations with size. It is well known that in the nanometric domain, the coercivity of the particles tends to zero.[23] Thus, the nanocrystals behave as superparamagnets with no associated coercivity or retentivity. The blocking temperature which marks the onset of this superparamagnetism also increases with the nanocrystal size. Further, the magnetic moment per atom is seen to increase as the size of a particle decreases[25] (see Figure 7).

Chemical reactivity: The surface area of nanocrystals increases markedly with the decrease in size. Thus, a small metal nanocrystal of 1 nm diameter will have ~100% of its atoms on the surface. A nanocrystal of 10 nm diameter on the other hand, would have only 15% of its atoms on the surface. A small nanocrystal with a higher surface area would be expected to be more reactive. Furthermore, the qualitative change in the electronic structure arising due to quantum confinement in small nanocrystals will also bestow unusual catalytic properties on these particles, totally different from those of the bulk metal. We illustrate these important aspects with a few examples from the recent literature.

A low temperature study[26] of the interaction of elemental O_2 with Ag nanocrystals of various sizes (Figure 8) has

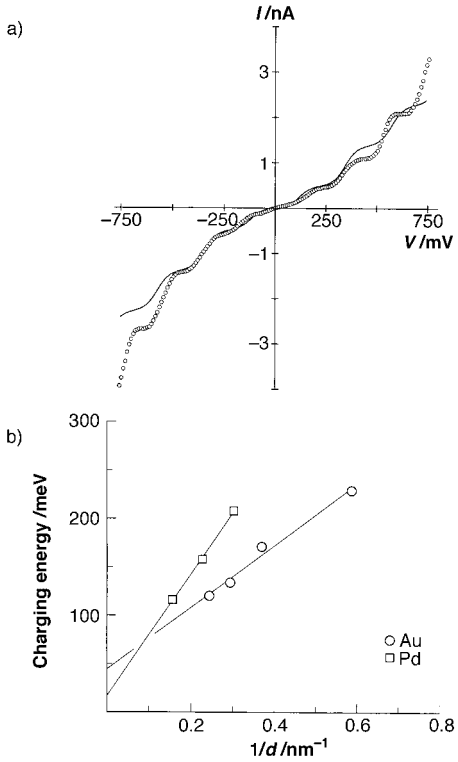

Figure 6. a) I-V characteristics of an isolated 3.3 nm Pd nanocrystal (dotted line) and the theoretical fit (solid line) obtained at 300 K using a semiclassical model according to which, the observed capacitance (*C*) may be resolved into two components *C*1 and *C*2 and the resistance (*R*) into *R*1 and *R*2, such that $C = C1 + C2$, $R = R1 + R2$. For $C1 \ll C2$ and $R1 \ll R2$, the model predicts steps in the measured current to occur at critical voltages, $V_c = n_c e/(C + (1/C)q_0 + e/2)$, where q_0 is the residual charge. b) Variation of the charging energies of Pd and Au nanocrystals with inverse diameters (*d*) (reproduced with permission from ref. [22]).

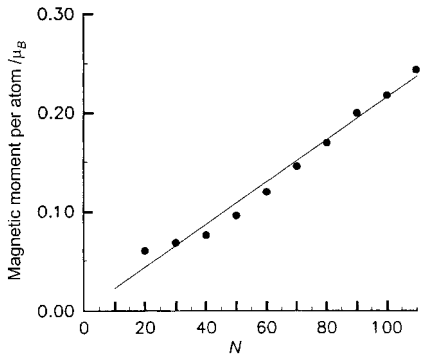

Figure 7. Variation of the magnetic moment per atom as a function of the number of atoms in Co clusters at $T = 170$ K and $H = 0.53\,T$. The continuous curve is the theoretical value and the solid circles are the experimental results (reproduced with permission from ref. [25b]).

0947-6539/02/0801-0032 $ 17.50+.50/0 *Chem. Eur. J.* **2002**, *8*, No. 1

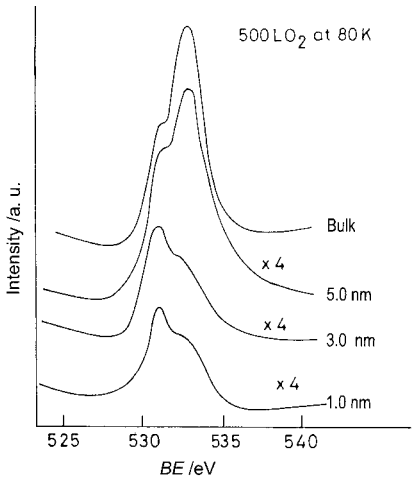

Figure 8. Change in the O(1s) spectra of Ag clusters exposed to 500 L O_2 at 80 K.The diameters of the clusters have been estimated from metal coverage. The lower binding energy peak at 531 eV corresponds to O^- while that at 533 eV arises due to molecular oxygen (reproduced with permission from ref. [26]).

revealed the capability of smaller nanocrystals to dissociate dioxygen to atomic oxygen species. On bulk Ag, the adsorbed oxygen species at 80 K is predominantly O_2^-. This interaction of O_2 with Ag—*dependent on its particle size*—is remarkable. Another important example is the reaction of H_2S with Ni nanocrystals giving rise to S^{2-} species, with nanocrystals of different sizes exhibiting different temperature profiles (see Figure 9). Unlike bulk nickel, small nanocrystals show less dependence in their catalytic activity on ambient temperature.

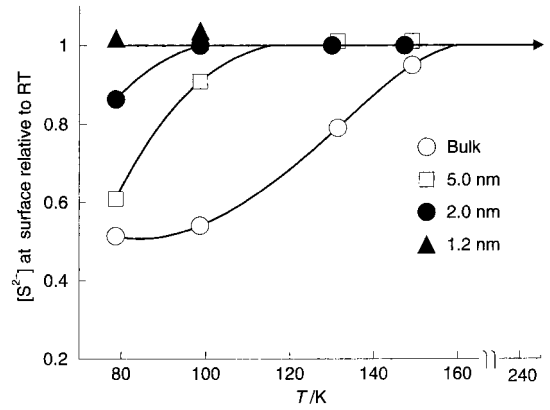

Figure 9. Variation of the normalized areas of the signal for the core-level transitions of S^{2-} with temperature for different sizes of Ni clusters deposited on graphite (reproduced with permission from ref. [26]).

The ability of Cu, Pd and Ni nanoparticles to absorb CO has been thoroughly investigated. Carbon monoxide from a bulk Cu surface desorbs above 250 K. Small Cu particles, however, retain CO up to much higher temperatures (Figure 10).[27] A similar observation has been made in case of Pd particles.[28] The results obtained with Ni particles are more even interesting. In addition to showing a trend similar to the above, small Ni particles are also capable of dissociating CO to form carbidic species on the particle surface (Figure 11).[29]

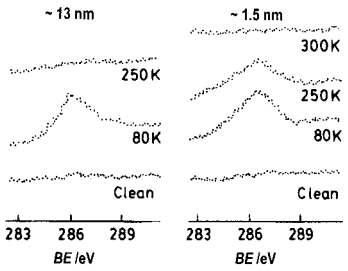

Figure 10. Change in the C(1s) spectra of CO adsorbed on Cu. The feature at 286 eV corresponds to molecularly adsorbed CO (reproduced with permission from ref. [27]).

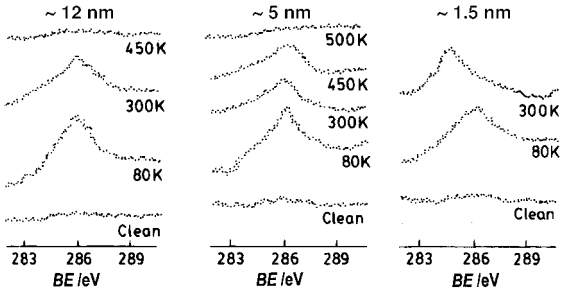

Figure 11. Change in the C(1s) spectra of CO adsorbed on Ni clusters with temperature. The feature at 286 eV corresponds to molecularly adsorbed CO while that at 284 eV arises due to the formation of carbidic species (reproduced with permission from ref. [27]).

This could be due to the Ni(3d) level in small clusters coming close to the anti-bonding energy level of CO($2\pi^*$).

Bulk Au is a noble metal. Goodman and co-workers,[30] however, found that Au nanocrystals supported on a titania surface show a marked size-effect in their catalytic ability for CO oxidation reaction, with Au nanoparticles in the range of 3.5 nm exhibiting the maximum chemical reactivity (Figure 12a). A metal to non-metal transition as observed in the I-V spectra (Figure 12b), as the cluster size is decreased below 3.5 nm^3 (consisting of ca. 300 atoms). This result is quite similar to that obtained with Pd particles supported on oxide substrate.[31] In another study of Au particles supported on a zinc oxide surface, smaller particles (<5 nm) exhibited a marked tendency to adsorb CO while those with diameters above 10 nm did not significantly adsorb CO (Figure 13).[32] The increased activity of these metal particles is attributed to the charge transfer between the oxide support and the particle surface.

Self-assembly of nanocrystals: Just as individual atoms aggregate to form crystals, nanocrystals themselves act as building units to form particle superlattices. Thus, monodispersed nanocrystals suitably covered by ligands such as alkane thiols, when transferred to a flat substrate, spontaneously assemble into two-dimensional lattices.[33–37] In Figure 14, we show typical arrays of 2.5 and 3.2 nm Pd nanocrystals coated with octane thiol. The diameter of the nanocrystal, *d*, and the length of the protecting ligand, *l*, play an important role in determining the very nature of the assembly.[38, 39] A study of the two-dimensional arrays formed by Pd nanocrystals of varying diameters covered with alkane thiols of different chain lengths has enabled to obtain an experimental stability

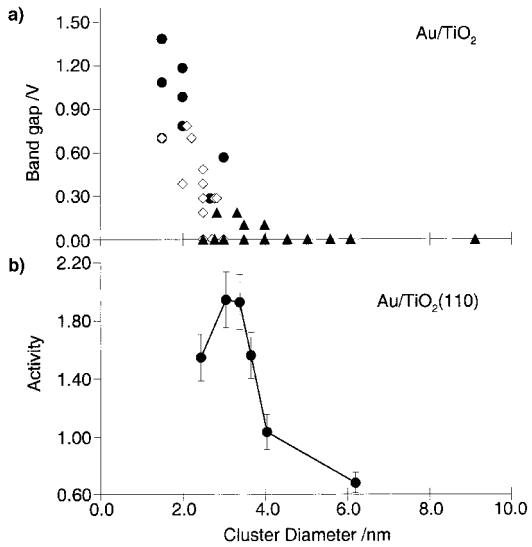

Figure 12. a) Cluster band gap measured by STS as a function of Au cluster size. The band gaps were obtained while the corresponding topographic scan was acquired on various Au coverages ranging from 0.2 to 4.0 ML. two-dimensional clusters ○; three-dimensional clusters, two atom layers in height □; three-dimensional clusters with three atom layers or greater in height △. b) The activity (*CO atoms/total Au atoms*) for CO oxidation at 350 K as a function of the Au cluster diameter supported on a TiO_2 surface. The CO/O_2 mixture was 1:5 at a total pressure of 40 Torr (reproduced with permission from ref. [30]).

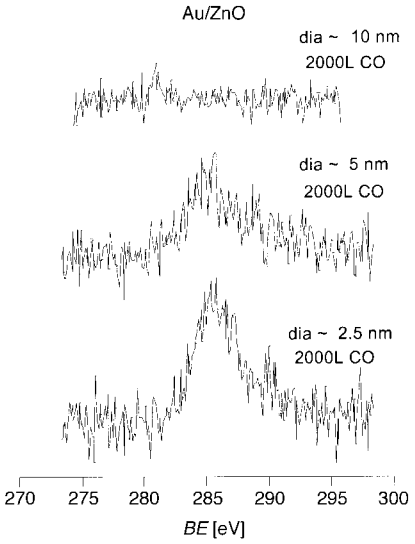

Figure 13. C(1s) core-level spectra of CO adsorbed on Au particles supported on a ZnO substrate. The feature at ~285 eV corresponds to molecularly absorbed CO. The diameters have been obtained from the metal coverages.

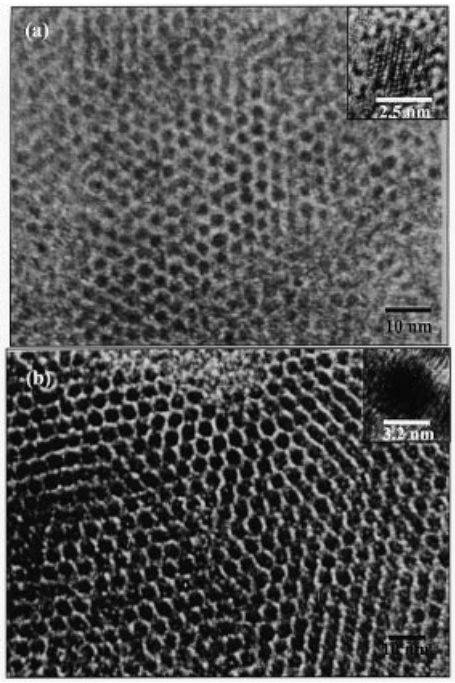

Figure 14. TEM micrograph showing hexagonal arrays of thiolized Pd nanocrystals: a) 2.5 nm, octane thiol, b) 3.2 nm, octane thiol (reproduced with permission from ref. [40]).

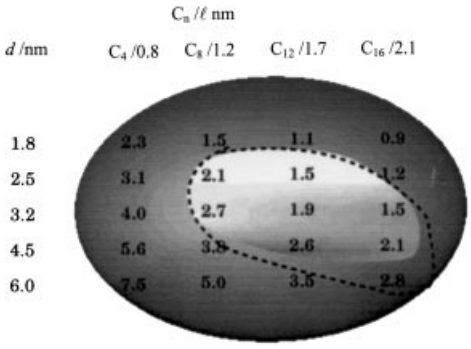

Figure 15. The $d-l$ phase diagram for Pd nanocrystals thiolized with different alkane thiols. The mean diameter, d, was obtained from the TEM measurements on as-prepared sols. The length of the thiol, l, is estimated by assuming an all-*trans* conformation of the alkane chain. The thiol is indicated by the number of carbon atoms, C_n. The bright area in the middle encompasses systems which form close-paced organizations of nanocrystals. The surrounding darker area includes disordered or low-order arrangements of nanocrystals. The area enclosed by the dashed line is derived from calculations from the soft sphere model (reproduced with permission from ref. [40]).

diagram (Figure 15) of the superlattices in terms of d and l.[40] In this Figure, the bright area in the middle is the most favourable d/l regime, corresponding to extended close packed organization, such as those illustrated in Figure 14. The d/l values for the most favorable regions are in the range 1.5 – 3.8. The area shaded dark in Figure 15 includes d/l regime giving rise to various short-range organizations; these are formed when the particles are small and the chain length is large or vice versa. The experimental results have been compared with empirical calculations based on a soft sphere model,[41] involving an attractive van der Waals term and a repulsive steric term (see Figure 15).

The ability to synthesize lattices of nanocrystals have led to explorations of their collective physical properties. Thus, it is observed in the case of Co nanocrystals (5.8 nm) that, accompanying lattice formation, the blocking temperature increases.[42] FePt alloy nanocrystals yield ferromagnetic assemblies for which the coercivity is tunable by controlling the parameters such as Fe:Pt ratio and the particle size.[43] The evolution of collective electronic states in CdSe nanocrystals have been followed by optical spectroscopic methods. Compared with isolated nanocrystals, those in the lattice exhibited

0947-6539/02/0801-0034 $ 17.50+.50/0 *Chem. Eur. J.* **2002**, *8*, No. 1

broader bands.[44] Various investigations have been carried out on the electrical transport properties of nanocrystalline lattices.[45, 46] Heath and co-workers have successfully demonstrated a reversible Mott–Hubbard metal–nonmetal transition with Ag nanocrystals (3 nm) capped with octane thiol.[47] Since then, this has been a subject of intense theoretical study.[48]

Conclusion

We have hitherto discussed in the earlier sections, electronic structure and properties, chemical reactivity and self-assembly of nanocrystals, particularly those of metals. The discussion should suffice to illustrate how size if a crucial factor in deciding the chemistry in the nano regime. These size dependent properties form the basis of nanoscience, where the properties are exploited for possible applications.

[1] a) J. S. Vermaak, L. W. Mays, D. Kuhlmann-Wilsdorf, *Surf. Sci.* **1968**, *12*, 128; b) G. Apai, J. F. Hamilton, J. Stohor, A. Thompson, *Phys. Rev. Lett.* **1979**, *40*, 165; c) A. A. Montano, G. K. Shenoy, E. E. Apl, W. Schulze, J. Urban, *Phys. Rev. Lett.* **1986**, *56*, 2076; d) H. J. Wasswemann, J. S. Vermaak, *Surf. Sci.* **1970**, *22*, 164; e) P. A. Buffat, J. P. Borel, *Phys. Rev. A* **1976**, *13*, 2287; f) W. P. Halperin, *Rev. Mod. Phys.* **1986**, *58*, 533.

[2] a) P. P.Edwards, R. L. Johnston, C. N. R. Rao in *Metal Clusters in Chemistry* (Eds.: P. Braunstein, G. Oro, P. R. Raithby), Wiley-VCH, **1998**; b) A. I. Kirkland, D. A. Jefferson, D. G. Duff, *Annual Reports C*, Royal Society of Chemistry, **1993**, p. 247.

[3] H. N. Aiyer, V. Vijayakrishnan, G. N. Subanna, C. N. R. Rao, *Surf. Sci.* **1994**, *313*, 392.

[4] a) D. C. Johnson, R. E. Benfield, P. P. Edwards, W. J. H. Nelson, M. D. Vargas, *Nature* **1985**, *314*, 231; b) Y. Volokitin, J. Sinzig, L. J. de Jongh, G. Schmid, M. N. Vargaftik, I. I. Moiseev, *Nature* **1996**, *384*, 624.

[5] V. Vijayakrishnan, A. Chainani, D. D. Sarma, C. N. R. Rao, *J. Phys. Chem.* **1992**, *96*, 8679.

[6] R. Busani, M. Folker, O. Chesnovsky, *Phys. Rev. Lett.* **1998**, *81*, 3836.

[7] K. Rademann, O. D. Rademann, M. Schlauf, V. Even, F. Hensel, *Phys. Rev. Lett.* **1992**, *69*, 3208.

[8] H. Haberland, B. von Issendrof, Y. Yufeng, J. Kolar, G. Thanner, *Z. Phys. D: At. Mol. Clusters* **1993**, *26*, 8.

[9] K. V. Sarathy, G. Raina, R. T. Yadav, G. U. Kulkarni, C. N. R. Rao, *J. Phys. Chem. B* **1997**, *101*, 9876.

[10] S. Link, M. A. El-Sayed, *J. Phys. Chem. B* **1999**, *103*, 4212.

[11] A. P. Alivisatos, *J. Phys. Chem.* **1996**, *100*, 13226.

[12] a) D. M. Mittleman, R. W. Schoenlein, J. J. Shiang, V. L. Colvin, A. P. Alivisatos, C. V. Shank, *Phys. Rev. B* **1994**, *49*, 14435; b) A. Henglein, *Ber. Bunsenges. Phys. Chem.* **1995**, *99*, 903.

[13] C. P. Vinod, G. U. Kulkarni, C. N. R. Rao, *Chem. Phys. Lett.* **1998**, *289*, 329.

[14] M. Miyake, T. Torimoto, T. Sakata, H. Mori, S. Kuwabata, H. Yoneyama, *Langmuir* **1997**, *13*, 742.

[15] M. Rosenblit, J. Jortner, *J. Phys. Chem.* **1994**, *98*, 9365.

[16] R. A. Perez, A. F. Ramos, G. L. Malli, *Phys. Rev. B* **1989**, *39*, 3005.

[17] O. D. Haberlen, S. C. Chung, M. Stener, N. J. Rosch, *J. Chem. Phys.* **1997**, *106*, 5189.

[18] S. H. Yang, D. A. Drabold, J. B. Adams, A. Sachdev, *Phys. Rev. B* **1993**, *47*, 1567.

[19] P. E. Lippens, M. Lannoo, *Phys. Rev. B* **1989**, *39*, 10935.

[20] C. P. Collier, T. Vossmeyer, J. R. Heath, *Annu. Rev. Phys. Chem.* **1998**, *49*, 371.

[21] Single Charge Tunneling, Coulomb Blockade Phenomena in Nanostructures (Eds.: H. Grabert, M. H. Devoret), *NATO-ASI Ser. B* **1992**, *294*.

[22] P. J. Thomas, G. U. Kulkarni, C. N. R. Rao, *Chem. Phys. Lett.* **2000**, *321*, 163.

[23] J. Jortner, *Z. Phys. D: At. Mol. Clusters* **1992**, *24*, 247.

[24] C. P. Bean, J. D. Livingston, *J. Appl. Phys.* **1959**, *30*, 1208.

[25] a) Van de Heer, P. Milani, A. Chatelain, *Z. Phys. D: At. Mol. Clusters* **1991**, *19*, 241; b) S. N. Khanna, S. Linderoth, *Phys. Rev. Lett.* **1991**, *67*, 742.

[26] C. N. R. Rao, V. Vijayakrishnan, A. K. Santra, M. W. J. Prins, *Angew. Chem.* **1992**, *104*, 1110; *Angew. Chem. Int. Ed. Engl.* **1992**, *31*, 1062.

[27] A. K. Santra, S. Ghosh, C. N. R. Rao, *Langmuir* **1994**, *10*, 3937.

[28] E. Gillet, S. Channakhone, V. Matolin, M. Gillet, *Surf. Sci.* **1986**, *152/153*, 603.

[29] a) D. L. Doering, J. T. Dickinson, H. Poppa, *J. Catal.* **1982**, *73*, 91; b) D. L. Doering, H. Poppa, J. T. Dickinson, *J. Catal.* **1982**, *73*, 104.

[30] M. Valden, X. Lai, D. W.Goodman, *Science* **1998**, *281*, 1647.

[31] C. Xu, X. Lai, G. W. Zajac, D. W. Goodman, *Phys. Rev. B* **1997**, *56*, 13464.

[32] Unpublished results from our laboratory.

[33] C. N. R. Rao, G. U. Kulkarni, P. J. Thomas, P. P. Edwards, *Chem. Soc. Rev.* **2000**, *29*, 27.

[34] A. N. Shipway, E. Katz, I. Willner, *Chem. Phys. Chem.* **2000**, *1*, 18.

[35] M. P. Pileni, *New J. Chem.* **1998**, 693.

[36] G. Schmid, L. F. Chi, *Adv. Mater.* **1998**, *10*, 515.

[37] W. P. Wuelfing, F. P. Zamborini, A. C. Templeton, X. Wen, H. Yoon, R. W. Murray, *Chem. Mater.* **2001**, *13*, 87.

[38] R. L. Whetten, M. M. Shafigullin, J. T. Khoury, T. G. Schaaf, I. Vezmar, M. M. Alvarez, A. Wilkinson, *Acc. Chem. Res.* **1999**, *32*, 397.

[39] P. C. Ohara, D. V. Leff, J. R. Heath, W. M. Gelbart, *Phys. Rev. Lett.* **1995**, *75*, 3466.

[40] P. J. Thomas, G. U. Kulkarni, C. N. R. Rao, *J. Phys. Chem. B* **2000**, *104*, 8138.

[41] B. A. Korgel, S. Gullam, S. Conolly, D. Fitzmaurice, *J. Phys. Chem. B* **1998**, *102*, 8379.

[42] a) V. Russier, C. Petit, J. Legrand, M. P. Pileni, *Phys. Rev. B* **2000**, *62*, 3910; b) C. Petit, M. P. Pileni, *Appl. Surf. Sci.* **2000**, *162–163*, 519; c) C. Petit, A. Taleb, M. P. Pileni, *Adv. Mater.* **1998**, *10*, 259.

[43] S. Sun, C. B. Murray, D. Weller, L. Folks, A. Maser, *Science* **2000**, *287*, 1989.

[44] a) M. V. Artemyev, A. I. Bibik, L. I. Gurinovich, S. V. Gopenko, U. Woggon, *Phys. Rev. B* **1999**, *60*, 1504; b) C. R. Kagan, C. B. Murray, M. G. Bawendi, *Phys. Rev. B* **1996**, *54*, 8633; c) M. V. Artemyev, U. Woggon, H. Jaschinski, L. I. Gurinovich, S. V. Gopenko, *J. Phys. Chem. B* **2000**, *104*, 11617.

[45] M. Brust, D. Bethell, D. J. Schiffrin, C. J. Kiely, *Adv. Mater.* **1995**, *7*, 795.

[46] a) D. B. Janes, V. R. Kolagunta, R. G. Osifchin, J. D. Bielefeld, R. P. Andres, J. I. Henderson, C. P. Kubiak, *Superlattices Microstruct.* **1995**, *18*, 275; b) A. W. Snow, H. Wohltjen, *Chem. Mater.* **1998**, *10*, 947; c) Y. Liu, Y. Wang, R. O. Claus, *Chem. Phys. Lett.* **1998**, *298*, 315; d) H. M. Jaeger, personal communication, **2001**.

[47] a) G. Markovich, C. P. Collier, S. E. Hendricks, F. Remacle, R. D. Levine, J. R. Heath, *Acc. Chem. Res.* **1999**, *32*, 415; b) C. Mederios-Riberio, D. A. A. Phlberg, R. S. Williams, J. R. Heath, *Phys. Rev. B* **1999**, *59*, 1633.

[48] F. Remacle, R. D. Levine, *Chem. Phys. Chem.* **2001**, *2*, 20.